RESEARCH ARTICLE

M. Otendal · O. Hemberg · T. T. Tuohimaa · H. M. Hertz

Microscopic high-speed liquid-metal jets in vacuum

Abstract The operation of microscopic high-speed liquid-metal jets in vacuum has been investigated. We show that such jets may be produced with good stability and collimation at higher speeds than previously demonstrated, provided that the nozzle design is appropriate and that cavitation-induced instabilities are avoided. The experiments with a medium-speed tin jet ($u \sim 60$ m/s, $\mathrm{Re} = 1.8 \times 10^4$, $Z = 2.9 \times 10^{-3}$) showed that it operated without any signs of instabilities, whereas the stability of high-speed tin jets ($d = 30$ μm, $u = 500$ m/s, $\mathrm{Re} = 5.6 \times 10^4$, $Z = 4.7 \times 10^{-3}$) has been investigated via dynamic similarity using a water jet. Such a 500-m/s tin jet is required as the anode for high-brightness operation of a novel electron-impact X-ray source.

Nomenclature

a	Nozzle radius
c_0	Speed of sound in the jet liquid
d	Jet diameter after contraction
d_0	Nozzle diameter
L	Jet break-up length
Ma	Mach number, jet-to-sound speed ratio
Re	Reynolds number, inertial-to-viscous force ratio
T	Temperature
u	Jet speed after contraction
u_0	Jet speed at the nozzle exit
We_A	Atmospheric Weber number, inertial-to-surface tension force ratio for the atmosphere
We_L	Liquid Weber number, inertial-to-surface tension force ratio for the jet liquid
Z	Ohnesorge number, viscous-to-surface tension force ratio
η_0	Initial disturbance amplitude on the jet
μ	Dynamic viscosity
ρ_A	Density of the atmosphere
ρ_L	Density of the jet liquid
σ	Surface tension

M. Otendal (✉) · O. Hemberg · T. T. Tuohimaa · H. M. Hertz
Biomedical and X-Ray Physics, Royal Institute of Technology,
KTH Albanova, 106 91 Stockholm, Sweden
E-mail: mikael.otendal@biox.kth.se

1 Introduction

We have investigated the stability of high-speed liquid-metal jets in vacuum. The study is motivated by the development of a new hard X-ray source (Hemberg et al. 2003, 2004), which requires a very fast ($\sim$500 m/s) microscopic ($\sim$30 μm) liquid-tin-jet anode. Unfortunately, only negligible information on high-speed metal jets in vacuum exist in the literature, and experimental data on any high-speed (> 100 m/s) jets in vacuum is very limited. In the present paper we show that liquid jets may be operated stably in vacuum at previously untested high speeds, provided that the nozzle design is appropriate and that cavitation-related instabilities are avoided.

Cylindrical liquid jets and their breakup have been described in several papers (McCarthy and Molloy 1974; Sterling and Sleicher 1975; Bogy 1979; Lin and Lian 1990; Blevins 1992; Leroux et al. 1996; Eggers 1997; Lin and Reitz 1998). Classically, they can be characterized by five dimensionless fluid-mechanical parameters:

$$\mathrm{Re} = \frac{\rho_L u_0 d_0}{\mu} \tag{1}$$

$$\mathrm{We}_L = \frac{\rho_L u_0^2 d_0}{\sigma} \tag{2}$$

$$Z = \frac{\sqrt{\mathrm{We}_L}}{\mathrm{Re}} = \frac{\mu}{\sqrt{\rho_L \sigma d_0}} \tag{3}$$

$$\mathrm{We}_A = \frac{\rho_A u_0^2 d_0}{\sigma} \tag{4}$$

$$\mathrm{Ma} = \frac{u_0}{c_0} \qquad (5)$$

Although the Ohnesorge number is not an independent parameter, it is of importance since it influences the development and growth of internal perturbations in the jet.

In atmospheric conditions, the breakup of a cylindrical liquid jet is classically divided into three main categories: Rayleigh breakup, wind-induced breakup, and sprays. At low speeds and small We_A, the jet breaks up into Rayleigh type, with uniformly spaced drops due to minimization of the surface energy. The wind-induced breakups are generated when the difference in relative speed between the jet and the ambient atmosphere is increased. This leads to aerodynamic pressure and viscous effects creating jet oscillations. If the jet speed is increased even further, the jet breakup is best described as a spray, where interaction with the atmosphere makes the jet disintegrate into very small droplets close to the nozzle orifice in a chaotic and irregular manner. The operation of the proposed high-speed tin jet (cf. data below) at atmospheric pressure would result in spray breakup. However, if the ambient pressure is reduced several orders of magnitude, the wind-induced breakup of the jet is not initiated (Fenn III and Middleman 1969; Phinney 1973). Thus, for a jet injected into vacuum, the break-up behavior is solely determined by the parameters of the nozzle geometry and the liquid, e.g., jet pinching by surface tension forces (McCarthy and Molloy 1974; Lin and Reitz 1998), velocity profile relaxation (McCarthy and Molloy 1974; Sterling and Sleicher 1975), and the vapor pressure of the liquid (Fuchs and Legge 1979; Muntz and Orme 1987).

At atmospheric pressure, streams of low-speed liquid-metal droplets have been operated in, e.g., solder machines (Wallace and Hayes 1997). In vacuum, continuous medium- and low-speed liquid-metal jets have been employed for the new X-ray source ($\sim$60 m/s) (Hemberg et al. 2003, 2004), laser-plasma experiments ($\sim$30 m/s) (Korn et al. 2002; Jansson et al. 2004), and for use in fusion reactors ($\sim$10 m/s) (Konkachbaev et al. 2000). However, to our knowledge, continuous high-speed ($>$100 m/s) metal jets have not been operated, neither in vacuum nor at atmospheric pressure. In the present paper we investigate the potential for operating such high-speed metal jets in vacuum and the stability issues involved. Owing to the difficulty of designing a system for generation of high-speed metal jets (requiring thousands of bars of pressure), we perform dynamic-similarity experiments (Douglas et al. 1995) using water jets to be able to predict the stability of future tin jets. The results are important for the new X-ray source, where a high speed of a microscopic liquid-tin anode directly translates into a potentially higher-brightness X-ray source facilitating improved-resolution X-ray imaging (Hemberg et al. 2003, 2004). The positional stability of the anode jet is also of utmost importance, since a stable X-ray source is required to achieve high
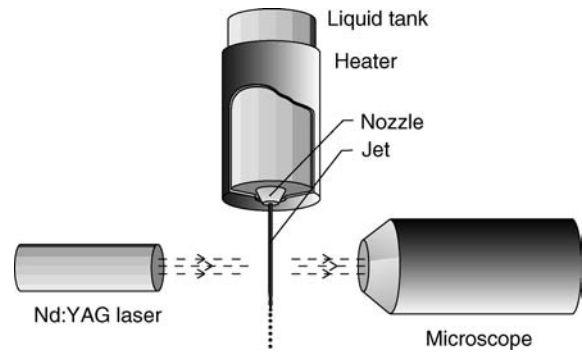

Fig. 1 Experimental arrangement

spatial resolution in X-ray imaging. Furthermore, increased understanding of the stability of high-speed liquid jets in vacuum is also important for improved high-repetition-rate operation of liquid-jet soft X-ray and extreme-ultraviolet laser-plasma sources (Rymell et al. 1995; Hansson et al. 2000).

2 Experimental arrangement

The liquid-jet system is shown in Fig. 1 and described in detail in Hemberg et al. (2003, 2004). It consists of a metal- or water-filled pressure tank, which is placed inside an IR-radiation heater capable of raising the temperature to $>$350°C. The pressure tank is placed in a vacuum chamber. The vacuum pressure can reach levels $<10^{-6}$ mbar. An external nitrogen-gas cylinder is connected to the pressure tank and provides up to 200 bars of backing pressure. Before the liquid is ejected through a nozzle into the vacuum, it passes through a stainless-steel particle filter. The nozzles are short (aspect ratios between 0.7 and 3.4) circular orifices made from ruby (sharp-edged straight hole) or sapphire plates (cone-shaped inlet followed by a straight section), see Table 1. Three different liquids were used in the experiments: 99.8% tin, deionized water, and deionized and particle-filtered water. The jets are collected in a tube, which could be cooled by liquid nitrogen for the water jets to reduce evaporation and maintain the vacuum. The jet is backilluminated by a 20-Hz, 4-ns pulsed frequency-doubled Nd:YAG laser, and imaged by a 12× zoom microscope. The maximum speed of the liquid-tin jet with the present system is $\sim$60 m/s. Collimated jets with diameters of 20–80 μm are readily produced and showed no signs of instability in the accessible speed/diameter range prior to the Rayleigh-breakup point. Figure 2 depicts a typical tin jet with its characteristic Rayleigh breakup.

3 Results and discussion

In this section the stability of low- and medium-speed tin jets are explored up to the limits of our experimental system. To simulate the behavior of high-speed tin jets,

Table 1 Nozzle parameters

	Nozzle type	Material	Diameter	Total length	Straight section	Inlet angle
1	Straight	Ruby	75 μm	254 μm	–	–
2	Straight	Ruby	356 μm	254 μm	–	–
3	Cone-shaped inlet, then straight	Sapphire	356 μm	1200 μm	254 μm	85°

we investigate water jets with matching fluid-mechanical dimensionless numbers. Finally, the validity of these experiments and the influence of nozzle design are investigated.

3.1 Low- and medium-speed tin jets

Figure 3 shows the break-up length of a liquid-tin jet ($Z = 2.9 \times 10^{-3}$), injected into a vacuum of $\sim 10^{-5}$ mbar, in terms of nozzle diameters as a function of Re. The experiment was performed with nozzle #1 and shows a steadily growing break-up length up to the maximum speed of our system at $Re = 1.8 \times 10^{4}$. The insert shows the qualitative classical break-up-length graph (Grant and Middleman 1966), where the arrow indicates the end of the Rayleigh-breakup zone. This point, commonly referred to as the critical speed or the critical point, has often been reported to be in the range $500 < Re < 3000$ (Phinney 1972; Blevins 1992), but values up to 10,000 have also been published (Grant and Middleman 1966). The break-up length at jet speeds below the critical speed is determined by (Phinney 1972)

$$\frac{L}{d_0} = \ln\left(\frac{a}{\eta_0}\right)\sqrt{We_L}(1+3Z),\qquad(6)$$

where the factor $\ln(a/\eta_o)$ is a measure of the initial perturbation of the jet and depends on a number of

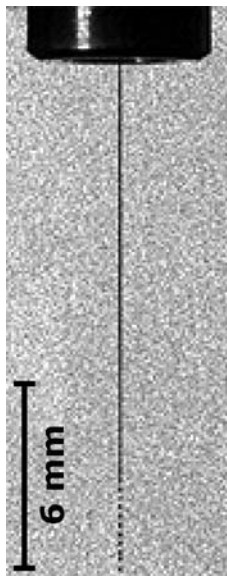different factors, e.g., nozzle design and system vibrations. From the jet-breakup experiment depicted in Fig. 3, a value of 13.5 is calculated for this factor for the tin jets. This is comparable to the values between 12 and 13.4 found in previous investigations (Smith and Moss 1917; Weber 1931; Grant and Middleman 1966; Blaisot and Adeline 2003). Thus, the tin jet can be operated at high Re ($\sim 18,000$) without any indication of reaching the critical speed. The plausible reason for this is that the combination of experimental parameters, e.g., low Ohnesorge number, short nozzle, and jet propagation through vacuum, places the jet in what is referred to as "zone 1" by Leroux et al. (1996), where the breakup is not influenced by the ambient atmosphere. The critical speed for the jets of this type is instead determined by the velocity profile relaxation and other instabilities inside the jet, e.g., turbulence. The results indicate that the critical velocity of microscopic tin jets in vacuum can be very high, which makes stable high-speed operation feasible. Such high-speed jets are investigated by means of dynamic similarity experiments in Sect. 3.2.

3.2 Simulation of high-speed tin jets

The fluid-mechanical parameters of the future 500-m/s liquid-tin jet are $Re = 5.6 \times 10^{4}$, $Z = 4.7 \times 10^{-3}$, $We_L = 7.0 \times 10^{4}$, $We_A \sim 10^{-7}$, and $Ma = 0.16$. These
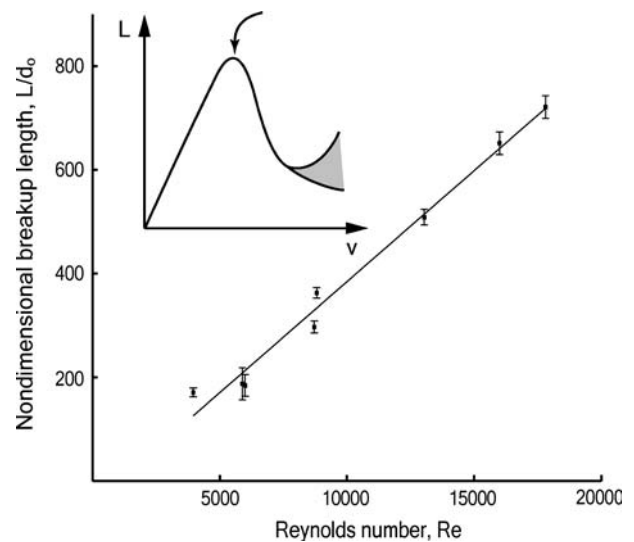

Fig. 2 Flash photograph of a ~ 30-m/s, ~ 50-μm diameter tin jet in vacuum

Fig. 3 Break-up curve for a ~ 75-μm diameter liquid-tin jet operating in vacuum at speeds up to ~ 60 m/s. Error bars indicate 1 SD. The insert schematically depicts the classical stability graph for jets in atmospheric environments, with an arrow indicating the critical point

numbers are based on the following assumptions: $T = 260°C$, $u_o \sim 400$ m/s, $d_o = 33$ µm, $\rho_L = 7.0 \times 10^3$ kg/m^3 (Thresh et al. 1968), $\rho_A \sim 10^{-8}$ kg/m^3, $\mu = 1.7 \times 10^{-3}$ Ns/m^2 (Thresh and Crawley 1970), $\sigma = 0.54$ N/m (Ricci et al. 1997), and $c_o = 2.5 \times 10^3$ m/s (Markov 1975). With a jet-contraction factor of ~ 0.9 (Middleman and Gavis 1961), this will give the previously mentioned jet diameter of ~ 30 µm and jet speed of ~ 500 m/s. Assuming a nozzle discharge coefficient (Blevins 1992) close to unity makes a backing pressure of ~ 6000 bar necessary to achieve this jet speed. To simulate the behavior of a 500-m/s tin jet, water-jets (produced with nozzle #2) with the following parameters were studied: $T = 31°C$, $u_o = 120$ m/s, $d_o = 356$ µm, and $\rho_A = 6.4 \times 10^{-2}$ kg/m^3 (vacuum pressure ~ 50 mbar), which result in Re $= 5.6 \times 10^4$, $Z = 4.7 \times 10^{-3}$, We$_L = 7.0 \times 10^4$, We$_A \sim 4.6$, and Ma $= 0.08$. While Re and Z, and thus also We$_L$, match the liquid-tin jet perfectly, We$_A$ and Ma do not. This does, however, not influence our discussion since these values are below the thresholds where they start influencing the fluid-mechanical behavior of the jet. For We$_A$ below 5.3, the jet is practically unaffected by the atmosphere (Fenn III and Middleman 1969). For Ma less than 0.3 it is generally assumed that the fluid is incompressible and that the flow speed differs by $< 1\%$ from incompressible flow theory (Blevins 1992). Finally we note that both liquids are Newtonian in the pressure ranges of interest for the present experiments, which for water is up to 200 bar (Bett and Cappi 1965), and for tin up to about 6000 bar.

Figure 4a depicts a high-speed water jet at ~ 13.5 cm from the nozzle. We observe a coherent and stable jet with no visible breakups. However, a slight oscillation of the jet diameter was detected indicating turbulence in the
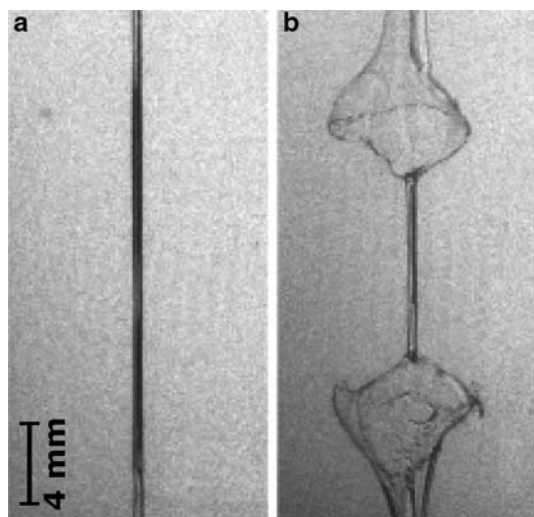

Fig. 4 Flash photographs of high-speed ~ 350-µm water jets in vacuum (~ 380 nozzle diameters from the nozzle exit). **a** No breakups occur when the vacuum pressure is higher than the vapor pressure of the water. **b** Reduction of vacuum pressure significantly below the vapor pressure of the water lead to bursting phenomena due to cavitation

jet flow. This is in agreement with the results in Sect. 3.3. The 13.5-cm distance equals ~ 380 nozzle diameters, which corresponds to ~ 13 mm for the future 30-µm high-speed tin jet. This is a sufficient distance to allow high-brightness operation of the future X-ray source that motivates this study.

When the ambient pressure was reduced to ~ 1 mbar, significantly below the vapor pressure of the water (~ 45 mbar), the jet becomes superheated as it enters the vacuum. For the deionized but not particle-filtered water, this leads to interesting break-up phenomena, as shown in Fig. 4b. The occurrence of these jet breakups is highly stochastic, but on average the break-up frequency is typically of a few Hertz. We believe that the phenomena are due to cavitation and rupture of the jet when heterogeneous nucleation is initiated at sites of microbubbles or particles in the water. In contrast, for the jets of deionized and particle-filtered water, the frequency of the ruptures is reduced by more than an order of magnitude, which is due to the substantially reduced concentration and size of the nucleation sites. It should, however, be noted that despite the experimental evidence in support of the nucleation and cavitation process, the break-up phenomena are not fully understood. Basically, the rupture of the jet should be related to the time for a bubble to grow large enough to destroy the jet (Muntz and Orme 1987). Thus, a slower jet should have breakups closer to the nozzle. However, when the water-jet speed was lowered below ~ 100 m/s ($d \sim 350$ µm, Re $\sim 35,000$) no ruptures could be detected in the observable range, suggesting that cavitation inside the nozzle is responsible for initiating the bursting phenomena, and therefore is removed by lowering the jet speed.

It is worth noting that cavitation-related bursting will not be an issue for a 30-µm tin jet due to a number of reasons. The vapor pressure for tin at 260°C is $\sim 10^{-20}$ mbar (Alcock 2001), which is many orders of magnitude below the operating vacuum pressure of the metal-jet hard X-ray source. Also, Muntz and Orme (1987) have shown that the minimum microbubble diameter that can lead to bubble growth inside a 30-µm diameter jet is larger than the jet diameter, unless the liquid temperature is substantially raised to achieve a very high vapor pressure. The conclusion is that microscopic tin jets are very unlikely to cavitate unless there are large quantities of dissolved gas in the tin. Thus, stable operation of very high-speed tin jets seems feasible.

3.3 Validity of dynamic-similarity experiments

In this section we investigate the validity of the high-speed dynamic similarity experiments by performing water-jet experiments in a fluid-mechanical parameter range where it can be compared with the tin jets in Sect. 3.1. The experimental arrangement allowed the studies of break-up lengths up to 35 cm, corresponding to
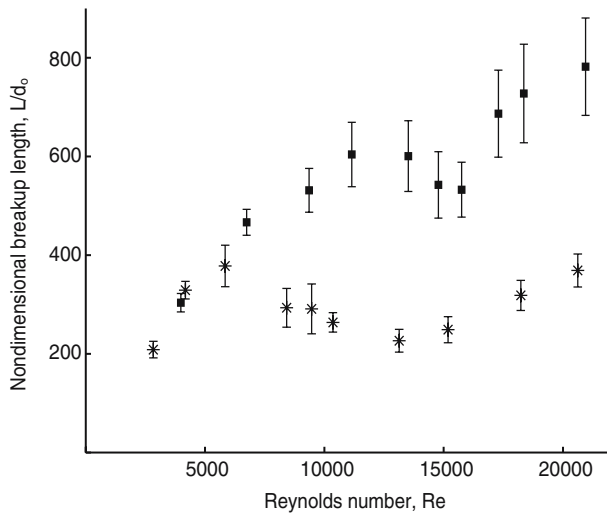
Fig. 5 Break-up curves for ~350-μm diameter water jets in "zone 1" using two different nozzles. Jet breakups for nozzle #2 are indicated with (■), and nozzle #3 with (*). Error bars indicate 1 SD

$Re = 2.1 \times 10^4$. Figure 5 shows the break-up length for deionized water for two different nozzles (#2 and #3). To ensure "zone 1" operation (cf. Sect. 3.1), both nozzles were short, the Ohnesorge number was low (and identical to the Z for a high-speed tin jet, 4.7×10^{-3}), and the jets were ejected into a 100-mbar vacuum, which puts We_A in the range 0.1–1.3. This is below the threshold value for atmospheric influence at $We_A = 5.3$ (Fenn III and Middleman 1969).

Although the break-up lengths for nozzles #2 and #3 in Fig. 5 follow the same principal behavior it is clear that the critical points differ (Re ~12,000 and ~6,000, respectively). These results can be compared with the critical point at Re > 18,000 for the tin jet produced with nozzle #1 (Sect.3.1). The Ohnesorge numbers are not identical, but still small enough for the stabilizing influence of the fluid viscosity to be negligible. The initial disturbances are small for all three nozzles ($\ln(a/\eta_0)$ is between 13 and 16), but still the critical velocity is significantly higher for nozzle #1 than the other nozzles. This shows that nozzle parameters such as inlet shape and nozzle aspect ratio are of great importance for the jet stability. Examples of how nozzle design influences jet stability have been discussed in several papers, e.g., Phinney and Humphries (1973); McCarthy and Molloy (1974); Sterling and Sleicher (1975); Leroux et al. (1997); and Blaisot and Adeline (2003).

The high-speed tin jet simulation in Sect. 3.2 was performed with nozzle #2, which clearly does not have the optimum design for stable jet generation. Still, it produces stable jets suitable for operation as anodes in the new type of hard X-ray source. Thus, we conclude that a 500-m/s, 30-μm tin jet, which was the target of this work, will be sufficiently stable. Finally, we note that a further improvement of jet stability will require optimization of nozzle design. Such improvement may lead to reduced jet-diameter fluctuations resulting in increased stability of the X-ray source.

4 Conclusions

In summary, the stability of high-speed liquid-metal jets in vacuum has been investigated. Stable operation of such jets is important for a more than 100-fold improvement of the brightness of future electron-impact hard X-ray sources. By means of dynamic similarity employing water jets, we conclude that a 30-μm liquid-tin jet anode may be operated stably in vacuum at ~500 m/s ($Re = 5.6 \times 10^4$ and $Z = 4.7 \times 10^4$). These experiments in combination with detailed break-up measurements suggest that the critical velocity for microscopic metal jets in vacuum can be very high, provided that the nozzle is appropriately designed to minimize turbulence. Finally we note that the major break-up mechanism of the water jet appears to be due to cavitation. However, the low vapor pressure of metal will make such cavitation-induced instabilities to be of negligible importance for the corresponding high-speed liquid-metal jet.

References

Alcock CB (2001) Vapor pressure of the metallic elements. In: Lide DR (eds) Handbook of chemistry and physics, 82nd edn, vol 4. CRC Press, New York, pp 4:134–136

Bett KE, Cappi JB (1965) Effect of pressure on the viscosity of water. Nature 207:620–621

Blaisot JB, Adeline S (2003) Instabilities of a free falling jet under an internal flow breakup mode regime. Int J Multiph Flow 29:629–653

Blevins RD (1992) Applied fluid dynamics handbook. Krieger Publishing Company, Malabar

Bogy DB (1979) Drop formation in a circular liquid jet. Annu Rev Fluid Mech 11:207–228

Douglas JF, Gasiorek JM, Swaffield JA (1995) Fluid Mechanics, 3rd edn. Longman Scientific& Technical, Singapore, pp 262–267

Eggers (1997) Nonlinear dynamics and breakup of free surface flows. Rev Mod Phys 69:865–928

Fenn III, RW, Middleman S (1969) Newtonian jet stability: The role of air resistance. AIChE J 15:379–383

Fuchs H, Legge H (1979) Flow of a water jet into vacuum. Acta Astronaut 6:1213–1226

Grant RP, Middleman S (1966) Newtonian jet stability. AIChE J 12:669–678

Hansson BAM, Rymell L, Berglund M, Hertz HM (2000) A liquid-xenon-jet laser-plasma x-ray and EUV source. Microel Engin 53:667–670

Hemberg O, Otendal M, Hertz HM (2003) Liquid-metal-jet anode electron-impact x-ray source. Appl Phys Lett 83:1483–1485

Hemberg O, Otendal M, Hertz HM (2004) Liquid-metal-jet anode x-ray tube. Opt Eng 43:1682–1688

Jansson PAC, Hansson BAM, Hemberg O, Otendal M, Holmberg A, de Groot J, Hertz HM (2004) Liquid-metal-jet laser-plasma extreme ultraviolet generation. Appl Phys Lett 84:2256–2258

Konkachbaev AI, Morley NB, Gulec K, Sketchley T (2000) Stability and contraction of a rectangular liquid metal jet in a vacuum environment. Fusion Eng Des 51–52:1109–1114

Korn G, Thoss A, Stiel H, Vogt U, Richardson M, Elsaesser T, Faubel M (2002) Ultrashort 1-kHz laser plasma hard x-ray source. Opt Lett 27:866–868

Leroux S, Dumouchel C, Ledoux M (1996) The stability curve of Newtonian liquid jets. Atom Sprays 6:623–647

Leroux S, Dumouchel C, Ledoux M (1997) The break-up length of laminar cylindrical liquid jets. Modification of Weber's theory. Int J Fluid Mech Res 24:428–438

Lin SP, Lian ZW (1990) Mechanisms of the breakup of liquid jets. AIAA J 28:120–126

Lin SP, Reitz RD (1998) Drop and spray formation from a liquid jet. Annu Rev Fluid Mech 30:85–105

Markov BG (1975) The speed of ultrasound and the thermophysical properties of the liquid metals Sn, Pb, Cd and of their binary alloys Pb-Sn and Pb-Cd. High Temp 13:1027–1030

McCarthy MJ, Molloy NA (1974) Review of stability of liquid jets and the influence of nozzle design. Chem Eng J 7:1–20

Middleman S, Gavis J (1961) Expansion and contraction of capillary jets of Newtonian liquids. Phys Fluids 4:355–359

Muntz EP, Orme M (1987) Characteristics, control, and uses of liquid streams in space. AIAA J 25:746–756

Phinney RE (1972) Stability of a laminar viscous jet–The influence of the initial disturbance level. AIChE J 18:432–434

Phinney RE (1973) Stability of a laminar viscous jet–The influence of an ambient gas. Phys Fluids 16:193–196

Phinney RE, Humphries W (1973) Stability of a laminar jet of viscous liquid–Influence of nozzle shape. AIChE J 19:655–657

Ricci E, Nanni L, Vizza M, Passerone A (1997) Dynamic surface tension measurements of liquid metals. In: Eustathopoulos N, Sobczak N (eds) Proceedings of international conference on high temperature capillarity, pp 188–193

Rymell L, Berglund M, Hertz HM (1995) Debris-free single-line laser-plasma x-ray source for microscopy. Appl Phys Lett 66:2625–2627

Smith SWJ, Moss H (1917) Mercury jets. Proc Roy Soc A 93:373–393

Sterling AM, Sleicher CA (1975) The instability of capillary jets. J Fluid Mech 68:477–495

Thresh HR, Crawley AF (1970) The viscosities of lead, tin, and Pb-Sn alloys. Metall Trans 1:1531–1535

Thresh HR, Crawley AF, White DWG (1968) The densities of liquid tin, lead, and tin-lead alloys. Trans Metall Soc AIME 242:819–822

Wallace DB, Hayes DJ (1997) Solder jet technology update. Proc SPIE 3235:681–684

Weber K (1931) Zum Zerfall eines Flüssigkeitsstrahles. Z angew Math Mech 11:136–159